

Theory of oscillatory firing induced by spatially correlated noise and delayed inhibitory feedback

Benjamin Lindner, Brent Doiron, and André Longtin

Department of Physics, University of Ottawa, 150 Louis Pasteur, Ottawa, Canada K1N-6N5

(Received 5 August 2005; revised manuscript received 14 October 2005; published 29 December 2005)

A network of leaky integrate-and-fire neurons with global inhibitory feedback and under the influence of spatially correlated noise is studied. We calculate the spectral statistics of the network (power spectrum of the population activity, cross spectrum between spike trains of different neurons) as well as of a single neuron (power spectrum of spike train, cross spectrum between external noise and spike train) within the network. As shown by comparison with numerical simulations, our theory works well for arbitrary network size if the feedback is weak and the amount of external noise does not exceed that of the internal noise. By means of our analytical results we discuss the quality of the correlation-induced oscillation in a large network as a function of the transmission delay and the internal noise intensity. It is shown that the strongest oscillation is obtained in a system with zero internal noise and adiabatically long delay (i.e., the delay period is longer than any other time scale in the system). For a neuron with a strong intrinsic frequency, the oscillation becomes strongly anharmonic in the case of a long delay time. We also discuss briefly the kind of synchrony introduced by the feedback-induced oscillation.

DOI: [10.1103/PhysRevE.72.061919](https://doi.org/10.1103/PhysRevE.72.061919)

PACS number(s): 87.19.La, 05.40.-a, 87.19.Bb

I. INTRODUCTION

Collective oscillations of groups of neurons is a common behavior in diverse brain regions [1,2]. Neural oscillations are thought to play critical roles in varied neural coding schemes. Examples include the binding of visual scenes [3], the detection of relevant stimuli [4–6], and position and velocity codes in the hippocampus [7]. Another frequent observation is that many neurons often “share” common fluctuations in both their membrane potential and spike trains [8]. These shared fluctuations can be induced by both common external stimuli [3] or shared internal projections [9]. Correlative relationships between collective oscillatory neural dynamics and shared single neuron fluctuations are common [3], yet direct causal mechanistic understandings are often elusive.

The authors and their colleagues have recently related neural population oscillations and shared fluctuations to the coding of natural scenes. Specifically, in weakly electric fish an oscillating firing activity in the first layer of information-processing neurons [pyramidal cells in the electrosensory lateral line lobe (ELL)] is present only if external stimuli are spatially extended [10] and sufficiently spatially correlated [11]. Put differently, the oscillation in the firing activity of pyramidal cells indicates the spatial structure of the stimulus. Electrosensory stimuli with these characteristics are representative of communication calls between fish; this is opposed to prey or background scene inputs which can be either spatially correlated or not [12].

In our past study [10] it was shown that a delayed inhibitory feedback pathway was critical for the stochastic oscillation observed in ELL pyramidal cells. That delayed feedback can result in oscillations is known for a long time [13]; the interplay between internal feedback and external correlations, however, has been addressed only rarely.

Analytical results on stochastic neural network oscillations are hard to achieve. Especially, the inclusion of an explicit delay in a stochastic system seems to lead to intractable

complications in the analysis, given that for stochastic delay systems even the determination of the stationary probability density equation is a hard problem [14,15]; temporal correlations that characterize an oscillatory activity pose in general an even greater calculational problem than the stationary probability density. Many researchers have analytically studied the population rate (population activity) of infinite networks, focusing in particular on the stability of neural activity (see, e.g., Refs. [16–24] and references therein). Two popular approaches are to treat the network dynamics by means of spike-response models in the framework of renewal theory [17,21] or by means of a stochastic mean field approach using the Fokker-Planck equation [16,18,23]. These approaches combined with the (mostly numerical) evaluation of the resulting equations have shown a rich variety of dynamical behavior in pulse-coupled networks. Within the framework of these theories, however, it has proven hard to obtain explicit expressions for the spectrum of the population rate. Furthermore, to our knowledge, no explicit results have been derived for single-neuron measures like the power spectrum (or autocorrelation function) of a single neuron or the cross spectrum (or cross correlation function) of two distinct neurons within the network. Finally, the problem of correlated stochastic input to a network (relevant in the aforementioned experiment in weakly electric fish and probably in a lot more cases) has been addressed to our knowledge only numerically for spiking neural systems [25–27] and theoretically for simplified uncoupled neural networks [28,29].

We have recently shown (Ref. [11]) that, for weak feedback, the spectral characteristics (characterizing oscillations as well as correlations in the network) can be related to single-neuron characteristics (power spectrum and susceptibility of a single uncoupled neuron) and network properties (coupling statistics, e.g., the feedback kernel) [11]. Our simple linear-response-like approach provided an explicit expression for the power spectrum of a single neuron in an infinite homogeneous network of stochastic leaky integrate-and-fire (LIF) neurons subjected to a global delayed feed-

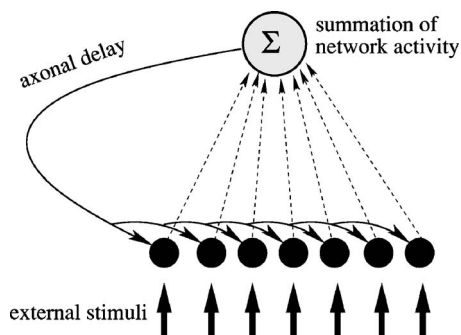


FIG. 1. The network model. Pyramidal cells (circles) receive correlated and uncorrelated external stimuli as well as inhibitory feedback of their spike trains. This feedback consists of the sum of all spike trains convoluted by an α function with time constant τ_S and delayed by a constant τ_D corresponding to the finite axonal transmission time.

back. The analytical solution described well the phenomenon of oscillations caused by the interaction of correlated stimuli and internal feedback in neural networks of weakly electric fish.

Our intentions in the present paper are as follows. First, we will generalize our theory to finite network size. We also develop expressions for other spectral quantities of interest which are accessible experimentally, such as the cross spectra between stimulus and single spike train or between the spike trains of distinct neurons. Furthermore, we want to explore the parameter space of the model including variations of system size, of the delay time, and of the internal noise intensity. We will show that an oscillation is already present for a single neuron and that the oscillation induced in a large network is enhanced by increasing the delay time and decreasing the internal noise intensity. We will also discuss the kind of synchrony in firing induced by the correlated input and the feedback, respectively.

Our paper is organized as follows. In Sec. II we introduce the neuron and network models as well as the spectral statistics we are interested in. In Sec. III we calculate the spectral measures for the case of a band-limited input stimulus (Sec. III A) and a white-noise stimulus of unlimited bandwidth (Sec. III B); in this section we also state the analytical results for a single leaky integrate-and-fire neuron (Sec. III C) that enable us to give explicit expressions for the spectral measures. Simulation results are compared to the theoretical ones in Sec. IV: the role of the network size will be studied in Sec. IV A; effects of varying the delay time and internal noise strength are explored in Sec. IV B; finally, the issue of network synchronization is addressed in Sec. IV C. We will summarize our results and draw some conclusions in Sec. V.

II. MODEL AND SPECTRAL STATISTICS

We consider a neural network with global inhibitory coupling as sketched in Fig. 1. The membrane voltage of the single neuron follows leaky-integrate-and-fire dynamics

$$\dot{v}_i = -v_i + I_i(t), \quad (1)$$

with $i=1, \dots, N$. Here time is measured in units of the membrane time constant, the resistance of the cell membrane is

lumped into the current, and the voltage variable and current are rescaled by a typical value such that all variables and parameters are nondimensional. The dynamics Eq. (1) is complemented by the well-known fire-and-reset rule: whenever the voltage reaches a prescribed constant threshold v_T , the neuron fires and the voltage is kept fixed for an absolute refractory period τ_R and then reset to a value v_R . In the following we set $v_T=1$ and $v_R=0$. The output of the i th LIF neuron is a δ spike train determined by the j th instants of threshold crossing of the i th neuron $t_{i,j}$

$$y_i(t) = \sum_j \delta(t - t_{i,j}). \quad (2)$$

The input current $I_i(t)$ consists of the following components [11]:

$$I_i(t) = \mu + \xi_i(t) + \sqrt{1-c} \eta_i(t) + \sqrt{c} \eta_c(t) + f(t). \quad (3)$$

The constant base current μ and the internal noise $\xi_i(t)$ of intensity D belong to the autonomous stochastic dynamics of the neuron itself. The internal noise processes of distinct neurons are Gaussian and uncorrelated (in time and among neurons)

$$\langle \xi_i(t) \rangle = 0, \quad \langle \xi_i(t) \xi_j(t') \rangle = 2D \delta_{i,j} \delta(t - t'). \quad (4)$$

The noise processes $\eta_i(t)$ and $\eta_c(t)$ are also uncorrelated among each other and represent the external inputs, which are specific for each or common to all neurons, respectively. The power spectrum of these processes is $S_{st}(\omega)$ [all processes $\eta_i(t)$, $\eta_c(t)$ share the same statistics]. We note that because of the scaling by the factors $\sqrt{1-c}$ and \sqrt{c} in Eq. (3) the total external input has a fixed intensity irrespective of the value of the correlation parameter c . The latter parameter can be varied between 0 and 1; c sets the spatial correlation coefficient of the external noise: for $c=0$ all external noise is uncorrelated among neurons whereas for $c=1$ each neuron receives an identical external stimulus.

The last term in Eq. (3) stands for the delayed inhibitory feedback of all spike trains generated by the network

$$f(t) = \frac{G}{N} \int_{\tau_D}^{\infty} d\tau \frac{\tau - \tau_D}{\tau_S^2} \exp\left[-\frac{\tau - \tau_D}{\tau_S}\right] \sum_{i=1}^N y_i(t - \tau). \quad (5)$$

This represents a convolution of the sum of all spike trains with a delayed α function. The feedback strength $G < 0$ is negative, indicating an inhibitory feedback; the decay time τ_S is related to the typical synaptic transmission time and is the inverse of the rate α used in our previous work [11]. Note that the arguments τ_D have been inadvertently omitted in Eq. (3) in [11].

In our modeling of pyramidal cells in the ELL of the weakly electric fish [10,11], the feedback kernel represents a distant neural population. This so-called NP nucleus receives the spikes generated by the ELL network and feeds them back after a convolution (corresponding mainly to the synaptic transmission to and from the distant population) and a transmission delay τ_D . We note that the above network dynamics applies to an even simpler situation, namely, to a network with delayed inhibitory all-to-all pulse coupling.

We will be mainly interested in the spectral statistics of the network. Introducing the Fourier transforms of the zero average spike trains

$$\tilde{y}_i(\omega) = \frac{1}{\sqrt{T}} \int_0^T dt e^{i\omega t} (y_i(t) - r_0), \quad (6)$$

we can determine the power spectrum of an arbitrary neuron's spike train and the cross spectrum between spike trains from two distinct neurons by

$$S(\omega) = \lim_{T \rightarrow \infty} \langle \tilde{y}_i \tilde{y}_i^* \rangle, \quad (7)$$

$$S_{cross}(\omega) = \lim_{T \rightarrow \infty} \langle \tilde{y}_i \tilde{y}_j^* \rangle, \quad j \neq i, \quad (8)$$

respectively (the asterix denotes the complex conjugate). Useful are also input-output relations like the cross spectrum between an arbitrary output spike train and the common part of the input noise

$$S_{i,o}(\omega) = \lim_{T \rightarrow \infty} \langle \tilde{y}_i \tilde{\eta}_c^* \rangle. \quad (9)$$

Finally, network properties can be characterized by the population activity

$$Y(t) = \frac{1}{N} \sum_{i=1}^N y_i(t) \quad (10)$$

or by the time-dependent behavior of the feedback kernel $f(t)$ (cf. Ref. [10]). It is easily found that the power spectrum of the population activity for a *homogeneous* network can be expressed by

$$S_{pop} = S_{cross} + \frac{1}{N} (S - S_{cross}), \quad (11)$$

while the feedback kernel possesses the power spectrum

$$S_{kern} = |F|^2 S_{pop} \quad (12)$$

$$= |F|^2 S_{cross} + \frac{|F|^2}{N} (S - S_{cross}), \quad (13)$$

where

$$F(\omega) = G \frac{e^{i\omega\tau_D}}{(1 - i\omega\tau_S)^2} \quad (14)$$

is the Fourier transform of the α function Eq. (5).

We see already here that, because of the mean-field-like scaling of the feedback kernel, both the population activity and the feedback kernel are dominated by the cross correlation between distinct output spike trains; other contributions enter only with $1/N$.

III. THEORY

The model as it is constitutes a highly nonlinear system (spiking neurons are per se nonlinear) that contains essential stochastic components as well as delayed feedback. Here we

present an analytical approach that allows to calculate spectral measures for a single neuron as it has been measured in experiments. The method works, as we will discuss below, reasonably well for neuron models with a moderate level of internal noise that linearizes their spectral transfer.

We assume that we know either exactly and by numerical simulations the characteristics of the neuron model with only internal noise, i.e., in open loop (no feedback, $G=0$) and in absence of external noise [$\eta_i(t) \equiv 0$, $\eta_c(t) \equiv 0$]. In particular, we need in the following the spontaneous firing rate $r = r_0(\mu, D)$, the power spectrum of the spike train $S_0(\omega, \mu, D)$, and the susceptibility $A(\omega, \mu, D)$ in open loop, where we indicate the parametric dependence of these functions on the base current μ and the internal noise intensity D . All these functions are known for a white-noise driven LIF with absolute refractory period τ_R [30,31] and will be explicitly stated in Sec. III C.

In this section we aim at relating the spectral characteristics introduced above to single-neuron properties (open-loop spectrum and susceptibility) and network properties (feedback kernel; delay time).

We will start in Sec. III A with the case of band-limited external noise sources. This case is conceptionally simple and will help to understand the more involved theory for the case of a unlimited white noise treated in Sec. III B. In Sec. III C we list the analytical results for the LIF that enable us to test explicit expressions of our theory against simulations of the network.

A. Theory for band-limited external stimuli

Here we assume that the external stimuli $\eta_i(t)$ and $\eta_c(t)$ have a small variance. This in turn requires a limited bandwidth for these stimuli, as for example, a band-limited white noise with small cutoff frequency or an Ornstein-Uhlenbeck process possessing a small variance. Thus the results derived here *do not* apply to the simple case of unlimited Gaussian white noise which has infinite variance; this latter case will be dealt with in the subsequent subsection.

Our first step is to split up the right-hand side of the neurons dynamics into an unperturbed part (leak term, base current, internal noise, and static feedback) and a perturbation (external stimuli and time-dependent part of the feedback)

$$I_i = \mu + \langle f(t) \rangle + \xi_i(t) + \frac{\sqrt{1-c}\eta_1(t) + \sqrt{c}\eta_c(t) + (f(t) - \langle f(t) \rangle)}{\quad} \quad (15)$$

Here $\langle f(t) \rangle$ is the stationary average of the feedback term or, in other words, the *static part* of the feedback. The underlined terms represent the time-dependent parts of external stimulus and feedback or, in other words, the perturbation. We assume that these parts are weak, i.e., that the standard deviation of all underlined terms is small compared to the base current μ . In particular, a single spike fed back through the kernel $F(t)$ cannot elicit a spike. Under these assumption, the stationary firing rate of the full system equals that of the unperturbed system which is an ensemble of independent stochastic spike generators with the effective base current $\mu' = \mu + \langle f \rangle$. Since the mean value of f is

$$\langle f \rangle = Gr \quad (16)$$

[the mean spike train $y_i(t)$ equals the stationary spike rate and the integral over the α function is one], the effective base current $\mu' = \mu + Gr$ and the firing rate can be found by solving the equation

$$r = r_0(\mu', D) = r_0(\mu + Gr, D), \quad (17)$$

where $r_0(\mu, D)$ is the stationary firing rate of a LIF neuron with base current μ , driven by white noise of intensity D .

With respect to the underlined terms in Eq. (15), we make the following linear response ansatz in the Fourier domain

$$\begin{aligned} \tilde{y}_i(\omega) = \tilde{y}_{0,i}(\omega) + A(\omega, \mu') & \left[\sqrt{1-c} \tilde{\eta}_i(\omega) + \sqrt{c} \tilde{\eta}_c(\omega) \right. \\ & \left. + \frac{F(\omega)}{N} \sum_{j=1}^N \tilde{y}_j(\omega) \right]. \end{aligned} \quad (18)$$

As for a linear system, we assume that the Fourier transform of the output equals that of the unperturbed system (denoted by $\tilde{y}_{0,i}$) plus a correction term consisting of the Fourier transform of the perturbative terms multiplied with the transfer function (i.e., the susceptibility). Our ansatz is similar to the so-called linear-fluctuation approximation [32]. Instead of using a deterministic dynamics that is weakly perturbed by noise, however, we extend the linear ansatz to a stochastic system (governed by a nonlinear dynamics and an internal noise) that is perturbed by external noise and by feedback.

In a linear system the transfer function is given by the susceptibility of the time-dependent mean value (of the spike train), which is $A(\omega)$. This is not strictly true even for weak perturbations since spike generators are nonlinear systems. If, however, the internal noise level D is sufficiently strong, we can expect that the error made with the ansatz is negligible because the internal noise linearizes the system with respect to external perturbations. See also Ref. [33] for a discussion of this issue for another kind of spike generator.

In the following we will use the fact that the unperturbed spike trains from distinct neurons are uncorrelated with each other and to the external stimulus, i.e.,

$$\langle \tilde{y}_{0,i} \tilde{y}_{0,j} \rangle = \langle \tilde{y}_{0,i} \tilde{\eta}_i^* \rangle = \langle \tilde{y}_{0,i} \tilde{\eta}_c^* \rangle = 0, \quad i \neq j. \quad (19)$$

Furthermore, since we deal with a homogeneous network, the statistics for all neurons are the same, e.g.,

$$\langle \tilde{y}_1 \tilde{y}_1 \rangle = \langle \tilde{y}_2 \tilde{y}_2 \rangle = \dots = \langle \tilde{y}_N \tilde{y}_N \rangle; \quad (20)$$

similarly, the cross spectra do not depend on the indices as long as these are different:

$$\langle \tilde{y}_1 \tilde{y}_2 \rangle = \langle \tilde{y}_1 \tilde{y}_3 \rangle = \dots \quad (21)$$

With these assumptions, it is possible to determine the spectral statistics from the linear ansatz. Multiplying Eq. (18) with

$$\tilde{y}_i^*, \tilde{y}_j^*, \tilde{y}_{0,i}^*, \tilde{y}_{0,j}^*, \tilde{\eta}_i^*, \tilde{\eta}_j^*, \text{ or } \tilde{\eta}_c^* \quad j \neq i$$

and averaging yields seven linear equations for the unknown quantities

$$\langle \tilde{y}_i \tilde{y}_i^* \rangle, \langle \tilde{y}_i \tilde{y}_j^* \rangle, \langle \tilde{y}_i \tilde{y}_{0,i}^* \rangle, \langle \tilde{y}_i \tilde{y}_{0,j}^* \rangle,$$

$$\langle \tilde{y}_i \tilde{\eta}_i^* \rangle, \langle \tilde{y}_i \tilde{\eta}_j^* \rangle, \langle \tilde{y}_i \tilde{\eta}_c^* \rangle \quad j \neq i.$$

These equations can be readily solved and after performing the limit $T \rightarrow \infty$ we obtain for the power spectrum

$$\begin{aligned} S = S_0 + |A|^2 S_{st} + c |A|^2 S_{st} \frac{2 \operatorname{Re}(AF) - |AF|^2}{|1 - AF|^2} \\ + \frac{1}{N} [S_0 + (1-c) |A|^2 S_{st}] \frac{2 \operatorname{Re}(AF) - |AF|^2}{|1 - AF|^2}, \end{aligned} \quad (22)$$

where $\operatorname{Re}(\cdot)$ indicates the real part.

Let us first discuss the infinite N limit where only terms in the first line survive. For $N \rightarrow \infty$, the spectrum consists of the unperturbed spectrum plus two correction terms. The first one stands for the transmitted signal power of the external stimulus—this term is expected for any driven system and has nothing to do with the feedback. The third term in Eq. (22) is proportional to the correlation parameter c and involves both response properties of the single neuron [i.e., $A(\omega)$] as well as network properties [i.e., $F(\omega)$]. For $c = 0$, $S(\omega)$ equals the power spectrum of the neuron driven solely by an external noise, i.e., the feedback has no effect in this case. The maximal feedback effect comes obviously into play with $c = 1$. The second correction term itself results from the correlation between spike train and the common part of the stimulus noise η_c [leading to the real part $\operatorname{Re}(AF)$] and from the correlation between different output spike trains (leading to the square $|AF|^2$). For weak feedback (small G , scaling the function F) the real part will be more important in shaping the power spectrum; hence, the correlations between spike train and input noise (input-output synchrony) is more relevant than the spike-spike correlation (network synchrony). This will be different for the population activity and the behavior of the feedback kernel. In the opposite limit of $N = 1$ we obtain

$$S = \frac{S_0 + |A|^2 S_{st}}{|1 - AF|^2}. \quad (23)$$

Here, the correlation parameter c becomes meaningless (there is only one stimulus) and consequently does not appear in the power spectrum anymore. The power spectrum is still influenced by the feedback, but with a multiplicative factor acting on the sum of spontaneous spectrum and transferred signal power rather than in an additive fashion.

Turning to other spectral measures for general N , we find for the correlation between an arbitrary output spike train and the common part of the input noise

$$S_{i,o} = \sqrt{c} \frac{AS_{st}}{1 - AF}. \quad (24)$$

The cross spectrum between the common part of the input noise and the output spike train is the only quantity that does not depend on N .

For the cross-spectrum between distinct output spike trains we obtain

$$S_{cross} = c|A|^2 S_{st} + c|A|^2 S_{st} \frac{2 \operatorname{Re}(AF) - |AF|^2}{|1 - AF|^2} + \frac{1}{N} (S_0 + (1 - c)|A|^2 S_{st}) \frac{2 \operatorname{Re}(AF) - |AF|^2}{|1 - AF|^2}. \quad (25)$$

The first term in the first line corresponds to the cross spectrum for two neurons that are driven by a common noise with spectrum cS_{st} ; such a term is also expected in linear response of a system without feedback. In the way we have written the cross spectrum it becomes apparent that the feedback terms (second term in the first line and the term in the second line) are exactly the same as for the power spectrum. Thus feedback and correlations [i.e., the function $F(\omega)$ and the parameter c] affect the auto and cross-correlation of the spike trains in the same way. This is so because spikes of distinct pulse trains and spikes of the same spike train are correlated through the same thing, namely, the oscillation of the feedback kernel. Put in the terminology of Ref. [10], the waves of inhibition arising periodically from the kernel correlate spikes (of different or of the same spike train) among each other. On top of that and on a short time-scale, auto- and cross correlations will be different because of refractoriness affecting the autocorrelation but not the cross correlation—this is reflected by the feedback-independent terms that differ in Eq. (22) and Eq. (25).

For large N we can neglect the second line in Eq. (25) and as for the feedback-related correction to the power spectrum, the cross spectrum between distinct spike trains is proportional to the correlation parameter. This implies that uncorrelated stimuli ($c=0$) do not induce any synchrony in a large network.

Using Eq. (11) together with Eq. (22) and Eq. (25), the population activity reads

$$S_{pop} = \frac{c|A|^2 S_{st}}{|1 - AF|^2} + \frac{1}{N} \frac{S_0 + (1 - c)|A|^2 S_{st}}{|1 - AF|^2} \quad (26)$$

and the power spectrum of the kernel is according to Eq. (12)

$$S_{kern} = \frac{c|FA|^2 S_{st}}{|1 - AF|^2} + \frac{|F|^2 S_0 + (1 - c)|A|^2 S_{st}}{N |1 - AF|^2}. \quad (27)$$

We note that one of the advantages of the theory as derived so far is that the effect of different spectral statistics $S_{st}(\omega)$ of the external input signal on the activity of the single neuron and on the network behavior can be studied. This remains an interesting subject for future investigations.

B. Theory for external white stimuli of unlimited bandwidth

Let us repeat what we have done so far. The static part of the feedback was included in the unperturbed system; we determined self-consistently the firing rate and the effective base current for this unperturbed system. Then we calculated in the spectral domain the linear response with respect to the external stimuli η_i , η_c and the feedback term. As pointed out above, the ansatz will work only for a small-variance external stimulus and a weak feedback, implying a finite cutoff frequency of the external stimulus or a sufficiently fast decay of the input spectrum at high frequencies.

Since in our work we are not interested in the effects of a finite cutoff frequency and a non-flat input spectrum, we can avoid making the small-signal assumption for the input noise as follows. We assume the external stimuli to be Gaussian white noise of intensity D_E , i.e.,

$$\langle \eta_c(t) \eta_c(t') \rangle = 2D_E \delta(t - t'),$$

$$\langle \eta_i(t) \eta_j(t') \rangle = 2D_E \delta_{i,j} \delta(t - t'), \quad i, j = 1, \dots, N. \quad (28)$$

For such a stimulus a linear correction of the spectral quantities is not valid anymore, because the variance of the white noise is not small but in fact infinite. For band-pass-limited external noise, a linear approximation of the effect of the external noise on the various quantities was reflected in terms like

$$S_0(\omega, D) + |A(\omega, D)|^2 S_{st} \quad (29)$$

(here we explicitly show the parametric dependence of the power spectrum and the susceptibility on the internal noise level). This is a linear approximation of

$$S_{0,Q} = S_0(\omega, Q), \quad (30)$$

where $Q = D + D_E$ is the intensity of the summed internal and external noise sources. If both internal and external noises are white and Gaussian, the single neuron cannot “distinguish” between both kinds of noise and, thus, to replace Eq. (29) by Eq. (30) seems to be plausible. This also extends to the firing rate and the susceptibility functions that should be taken at noise intensity Q and not at D anymore. As a matter of fact, an external stimulus treated by the strict linear response in Eq. (29) will never affect the stationary firing rate of the neuron. In contrast to this we expect an increase in firing rate for a neuron that experiences a white noise of total intensity $Q = D + D_E$ compared to the unperturbed case ($D_E = 0$). Replacing Eq. (29) by Eq. (30) and also taking the susceptibility $A(\omega, D)$ at the full noise level Q instead of D [i.e., using $A_Q = A(\omega, Q)$ in all expressions] reduces our linear response result with respect to both external noise and feedback to a linear response with respect to only the feedback term. For the self-consistent determination of the firing rate we also use the full noise intensity Q instead of D , i.e., we solve

$$r = r_0(\mu + Gr, Q), \quad (31)$$

where r_0 is the functional dependence of the firing rate on the base current at the noise level Q .

Using this approximation, our results for the single-neuron spectrum and the input-output cross spectrum read

$$S = S_{0,Q} + \left[2cD_E |A_Q|^2 + \frac{S_{0,Q} - 2cD_E |A_Q|^2}{N} \right] \times \frac{2 \operatorname{Re}(A_Q F) - |A_Q F|^2}{|1 - A_Q F|^2}, \quad (32)$$

$$S_{i,o} = 2\sqrt{c}D_E \frac{A_Q}{1 - A_Q F}. \quad (33)$$

Regarding the remaining spectral measures, we note that they all depend on the cross spectrum of distinct spike trains. Using only single neuron properties, the above replacement of $S_0(\omega) + 2D_E|A|^2$ by $S_{0,Q}(\omega)$ results in the following expressions for the cross spectrum of distinct spike trains, the spectrum of the population activity, and the spectrum of the feedback kernel

$$S_{cross} = 2cD_E \frac{|A_Q|^2}{|1 - A_Q F|^2} + (S_{0,Q} - 2cD_E|A_Q|^2) \times \frac{2 \operatorname{Re}(A_Q F) - |A_Q F|^2}{N|1 - A_Q F|^2}, \quad (34)$$

$$S_{pop} = 2cD_E \frac{|A_Q|^2}{|1 - A_Q F|^2} + \frac{S_{0,Q} - 2cD_E|A_Q|^2}{N|1 - A_Q F|^2}, \quad (35)$$

$$S_{kern} = 2cD_E \frac{|FA_Q|^2}{|1 - A_Q F|^2} + |F|^2 \frac{S_{0,Q} - 2cD_E|A_Q|^2}{N|1 - A_Q F|^2}. \quad (36)$$

A better approximation of these quantities can be certainly achieved when linear response is not used for the cross spectrum of the unperturbed system as it is in the above relations. The cross spectrum in the unperturbed case corresponds to that for a feedback-free system of two neurons driven by the effective base current μ' , a common noise, and independent noise sources, i.e., the input currents to the neurons are given by

$$I_i(t) = \mu' + \xi_i(t) + \sqrt{1-c}\eta_i(t) + \sqrt{c}\eta_c(t), \quad i = 1, 2. \quad (37)$$

The cross spectrum $S_{cross,0}(\omega)$ for these two neurons is not a single neuron property. Moreover, we are not aware of any stochastic neuron model for which an exact expression for this cross spectrum is known. Provided we know an expression or we measure it from a simulation of or experiment on two uncoupled neurons, we can use the following relations for a better approximation of the cross spectrum

$$S_{cross} = S_{cross,0} + \left(2cD_E|A_Q|^2 + \frac{S_{0,Q} - 2cD_E|A_Q|^2}{N} \right) \times \frac{2 \operatorname{Re}(A_Q F) - |A_Q F|^2}{|1 - A_Q F|^2}. \quad (38)$$

Using this relation together with Eq. (11) and Eq. (12) we can also calculate a better approximation for the spectra of the population activity and the feedback kernel. In the case of a more complicated neuron model for which none of the single neuron characteristics are analytically known, we could apply the achieved formulas as follows. By a simple simulation of the open-loop system (no feedback), we measure the unperturbed power spectrum, the firing rate, and the cross spectrum of two neurons; adding an external periodic signal we can also measure the susceptibility of the single neuron at a specific frequency. These curves can then be used by our theory to relate single-neuron characteristics (unperturbed power spectrum, susceptibility of the single neuron

and the unperturbed cross spectrum of two neurons that are driven by a common noise) and network properties (the kernel) to the spectral statistics of the network and of a single neuron within the network. The same holds for a real neuron for which the single neuron properties can be measured *in vitro*.

On the other hand, there are a few neuron models for which the needed quantities are analytically known. The most realistic of those models is the leaky integrate-and-fire (LIF) neuron with internal additive white-Gaussian noise. In the next subsection we briefly give the needed expressions for this model.

C. Needed analytical expressions for the LIF

For the LIF model we can calculate the firing rate by the following expression [34]

$$r_0(\mu, D) = \left(\tau_R + \sqrt{\pi} \int_{(\mu-v_T)/\sqrt{2D}}^{(\mu-v_R)/\sqrt{2D}} dz e^{z^2} \operatorname{erfc}(z) \right)^{-1}. \quad (39)$$

Furthermore, we know the power spectrum of the unperturbed system [30]

$$S_0(\omega, \mu, D) = r \frac{\left| \mathcal{D}_{i\omega} \left(\frac{\mu - v_T}{\sqrt{D}} \right) \right|^2 - e^{2\delta} \left| \mathcal{D}_{i\omega} \left(\frac{\mu - v_R}{\sqrt{D}} \right) \right|^2}{\left| \mathcal{D}_{i\omega} \left(\frac{\mu - v_T}{\sqrt{D}} \right) - e^{\delta} e^{i\omega\tau_R} \mathcal{D}_{i\omega} \left(\frac{\mu - v_R}{\sqrt{D}} \right) \right|^2}, \quad (40)$$

$$\delta = \frac{v_R^2 - v_T^2 + 2\mu(v_T - v_R)}{4D},$$

as well as the susceptibility of the system (Fourier transform of the linear response function) [31]

$$A(\omega, \mu, D) = \frac{ri\omega/\sqrt{D} \mathcal{D}_{i\omega-1} \left(\frac{\mu - v_T}{\sqrt{D}} \right) - e^{\delta} \mathcal{D}_{i\omega-1} \left(\frac{\mu - v_R}{\sqrt{D}} \right)}{i\omega - 1 \mathcal{D}_{i\omega} \left(\frac{\mu - v_T}{\sqrt{D}} \right) - e^{\delta} e^{i\omega\tau_R} \mathcal{D}_{i\omega} \left(\frac{\mu - v_R}{\sqrt{D}} \right)}. \quad (41)$$

The functions $\operatorname{erfc}(x)$ and $\mathcal{D}_a(z)$ are the complementary error function and the parabolic cylinder functions [35] that can be readily calculated with computer programs like MAPLE or MATHEMATICA.

IV. RESULTS: COMPARISON TO STOCHASTIC SIMULATIONS

Here we compare our analytical formulas to simulation results. We will be especially interested in what happens to the feedback-induced oscillation at different network sizes, internal noise strength, and values of the correlation parameter c .

The simulations we shall present in this section were obtained as follows. We simulated between 10^2 and 10^3 realizations (depending on network size) with a time step of $\Delta t = 5 \times 10^{-4}$. The internal noise source was simulated as an

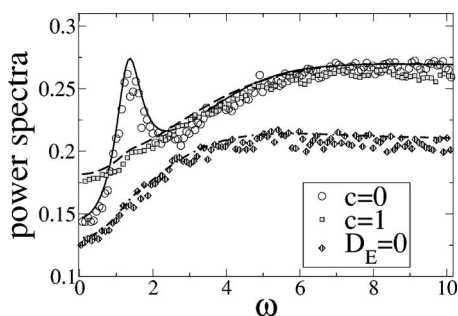


FIG. 2. Power spectrum of a single neuron in a network of $N=100$ neurons for $c=0$ (squares, dashed lines) and $c=1$ (circles, solid lines); simulations (symbols) compared to theory Eq. (32). Parameters are $D=0.12$, $G=-1.2$, $\mu=0.8$, $\tau_R=0.1$, $D_E=0.08$, $\tau_S=0.5$, and $\tau_D=1$.

unlimited white Gaussian noise (see, e.g., Ref. [36], Chap. 3.6) using a simple Euler procedure. For the external noise we used either a bandpass-limited Gaussian noise with a high cutoff frequency of $F_{cut}=70$ (Sec. IV A) or also an unlimited white Gaussian noise (remaining subsections). We chose a bandpass-limited noise in order to facilitate the calculation of cross spectra between input and output in Sec. IV A.

As shown in [11], a sufficiently strong feedback-coupling together with a spatial correlation of the external stimulus results in a pronounced oscillation in the firing activity of a single neuron embedded in the network. This is demonstrated in Fig. 2 for a large network comparable to the situation discussed in [11]. For $c=1$ (entirely correlated external stimulus), a peak around $\omega=1.5$ appears and the power at low frequencies is considerably reduced. Both effects are due to the delayed feedback in combination with the spatial correlations. In fact, the correction to the unperturbed power spectrum in Eq. (32) (for $N \rightarrow \infty$) is zero if either the spatial correlation ($c=0$) or the feedback [$G=0$ in $F(\omega)$] vanishes. The case of vanishing correlations ($c=0$) is shown in Fig. 2: the peak around $\omega=1.5$ vanishes and the power spectrum has more power at low frequencies ($\omega < 1$). To furthermore demonstrate that the oscillation is *not impeded* by the external noise, we also show in Fig. 2 the power spectrum in the absence of *any* external stimulus ($D_E=0$). In this case, not only the spectral peak is absent but also the overall spectrum is reduced because of the drop in firing rate when the external noise is switched off.

A. Finite size network: Spectral measures

We now explore whether the network and the spatial correlations are necessary for this effect and which kinds of finite-size effects may be observed.

We choose a small bias current $\mu=0.8$ such that even without feedback the neurons are in a subthreshold firing regime, i.e., spikes are solely induced by internal or external noise. Furthermore, we use a large internal noise intensity ($D=0.12$) and a weak feedback ($G=-0.5$; note that this is considerably smaller than in Fig. 2). In Fig. 3 we show data for a single neuron ($N=1$), a small “network” ($N=2$), and a large network ($N=100$). As it turns out, the oscillation indi-

cated by a low-frequency peak in the power spectrum (upper row) is present already for a single neuron (left panel). We postpone our discussion of the dependence of single spike train spectrum on system size until we have covered the spectra of the population, kernel, and the cross spectrum.

The power spectra of the output of the feedback kernel (fourth row in Fig. 3) and of the population rate (fifth row in Fig. 3) show a peak at finite frequency corresponding to the feedback-induced oscillation. Because of the low-pass-filter property of the kernel the oscillation peak is more clearly visible in $S_{kern}(\omega)$ and in $S_{pop}(\omega)$ than in $S(\omega)$. Remarkably, the distinction between $c=0$ and $c=1$ for a small network (mid panel) is much more pronounced than in the power spectrum of the spike train. For a large network ($N=100$, right panel), a peak remains only for $c=1$ but not for $c=0$. Generally, even for $c=1$ the oscillation peak decreases with system size.

The cross spectrum between different output spike trains for $N=2$ and $N=100$ is shown in the lowest row in Fig. 3. Because of symmetry, this spectrum is purely real. For $N=2$ there is a remarkable difference between the correlated and the uncorrelated case. For $c=1$ the cross spectrum is positive for all frequencies with a peak at the oscillation frequency. In contrast, for $c=0$ the cross spectrum can be both positive and negative. This is reasonable because in this case the neurons are not driven by the same external noise anymore, and the correlation between different output spike trains relies entirely on the feedback. The difference between the cross spectra for $c=0$ and $c=1$ is much more pronounced for a large network ($N=100$, right panel). Only for $c=1$ is a noteworthy correlation observed, while for $c=0$ the correlation among different spike trains is close to zero.

We now return to the oscillatory nature of the single spike train as indicated by the pronounced peak in $S(\omega)$ (top row in Fig. 3). In particular, we note that the peak is most impressive for a network with only one neuron ($N=1$), and reduces as N increases. This drop, however, does not continue further on increasing N , i.e., the power spectrum for $N=100$, is roughly the same as the one we would get for $N=1000$.

The decrease of the feedback-induced peak with system size is due to the way we scaled the system. To elaborate, the influence of a spike train on the dynamics of the neurons in the network is strongest when $N=1$. As N increases the influence of a given spike train is diluted by the presence of other spike trains in the network. This scaling is needed to guarantee that the feedback term is weak for all N . This effective system size dilution reduces spike train–spike train synchrony as measured by $S_{cross}(\omega)$ (final row in Fig. 3). A reduction in system synchrony via an increase in N has two effects on oscillatory behavior. First, the feedback induced shaping of the spike train power spectrum is compromised due to a less temporally precise feedback term; this is evident by the reduction in $S_{kern}(\omega)$ with system size (fourth row in Fig. 3). However, the temporal average of the feedback is necessarily invariant with respect to N as given by Eqs. (18) and (32). Second, the capacity for stimulus-induced synchrony (via an increase in c) to shape single unit oscillatory behavior is enhanced. This is evident in that the small peak in $S(\omega)$ that is present for $c=1$ when $N=100$ vanishes com-

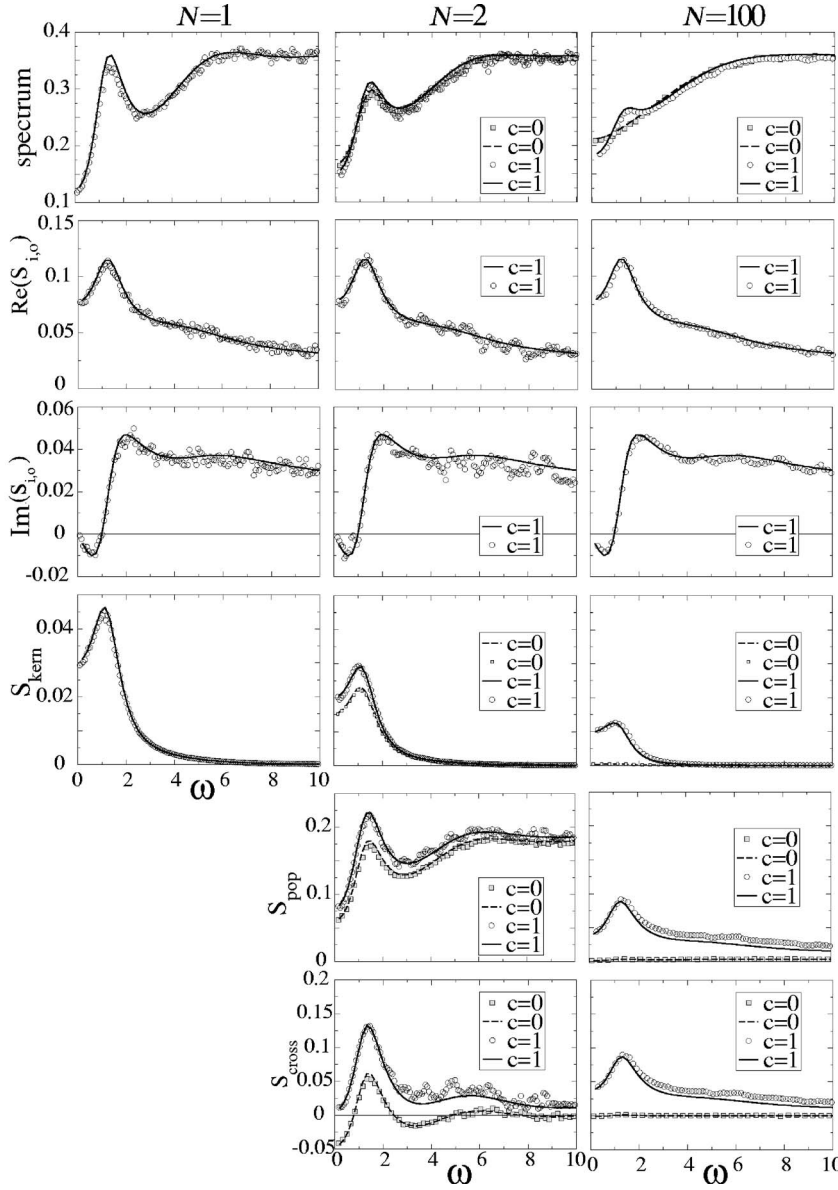


FIG. 3. Spectral measures obtained by simulations (symbols) compared to theory (lines) for $c=0$ (squares, dashed lines) and $c=1$ (circles, solid lines) and different system size N ; from top to bottom (with theoretical expressions given in brackets): power spectrum of a single neuron [Eq. (32)], real part and imaginary part of the cross spectrum between the common part of the external noise and the spike train of a single neuron [Eq. (33)], power spectrum of the feedback kernel [Eq. (36)], spectrum of the population activity [Eq. (35)], and cross spectrum between spike trains from distinct neurons [Eq. (34)]. Network size is $N=1$ (left column), $N=2$ (mid column), and $N=100$ (right column). Parameters are $\mu=0.8$, $D=0.12$, $D_E=0.08$, $G=-0.5$, $\tau_R=0.1$, $\tau_S=0.5$, and $\tau_D=1$.

pletely if $c=0$ and the power increases at low frequencies. The real and imaginary parts of the cross spectrum between common noise and output spike train are plotted in the second and third rows of Fig. 3. As predicted by the theory Eq. (33), this cross spectrum does not depend on the system size. The real part is roughly one order of magnitude larger than the imaginary part, indicating only a small phase shift between the output spike train and the common part of the external noise. We note that the agreement with the theory is excellent. Trivially, for $c=0$ this cross spectrum is zero (not shown).

The strongest deviations between theory and simulations are obtained for the cross spectrum between distinct spike trains at high frequencies. According to the discussion in Sec. III B, this was to be expected since we approximated the cross spectrum of the system without feedback also by linear response. As pointed out in that section, we may improve the approximation considerably if we know the cross spectrum for two uncoupled neurons ($G=0$) that are driven by an input current Eq. (37), i.e., by the effective base current (including

the effect of the static part of the feedback) and by common and internal noise sources. This is demonstrated in Fig. 4 for the data shown in the lowest row in Fig. 3. Indeed, using the cross spectrum of the two uncoupled neurons in Eq. (38), we achieve an excellent agreement between theory and simulation results. The improvement is mainly at high frequencies.

The ansatz Eq. (38) can be checked also in a different way. We may simulate the network *with* feedback but with a large value of the synaptic time constant τ_S . Such a small value in the synaptic rate constant τ_S^{-1} implies that the feedback is smeared out in time—there is no sharp delay anymore and for this reason we can expect that only the static part of the feedback survives. Hence, we predict that

$$S_{cross,0}(\omega, \mu', Q) = \lim_{\tau_S \rightarrow \infty} S_{cross}(\omega, \mu, Q). \quad (42)$$

A test for this limit as well as for our improved formula Eq. (38) is to use $S_{cross}(\omega, \mu, Q)$ in Eq. (38) evaluated at a large value of τ_S and to compare the result to the cross spectrum at a finite value of τ_S . This is done in Fig. 5, where we changed

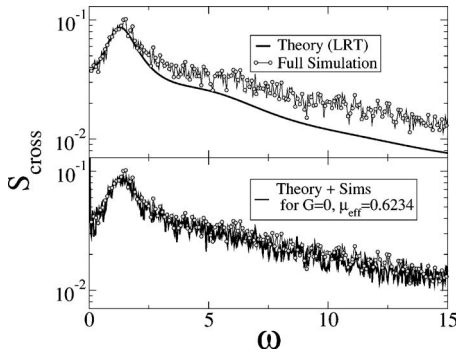


FIG. 4. Improved theory for the cross spectrum for $\mu=0.8$, $D=0.12$, $D_E=0.08$, $G=-0.5$, $\tau_R=0.1$, $\tau_S=0.5$, and $\tau_D=1$. Upper panel: The full simulation result (black) is compared to the purely theoretical result Eq. (34). This is a log plot of the data shown in Fig. 3 (right panel in lowest row). Lower panel: The same simulation result is compared to Eq. (38) where we have used the numerically computed spike train cross spectrum of two uncoupled neurons driven by currents given in Eq. (37) with $\mu'=0.6234$ (incorporating the static part of the feedback for $G=-0.5$). Since the latter cross spectrum was estimated by another simulation (of only two neurons), the corresponding “theory” curve is not smooth. Note the much better agreement in the lower panel.

the parameter values to demonstrate that the approach is valid also for stronger oscillation strength, i.e., where the cross spectrum shows many higher harmonics (see also the next subsection).

B. Large network: Oscillation frequency and degree of spectral coherence as functions of delay and internal noise

We now focus on a large network ($N=100$) and a correlated stimulus ($c=1$) of unlimited band-width. We study how the emerging oscillation depends on delay time and internal noise level.

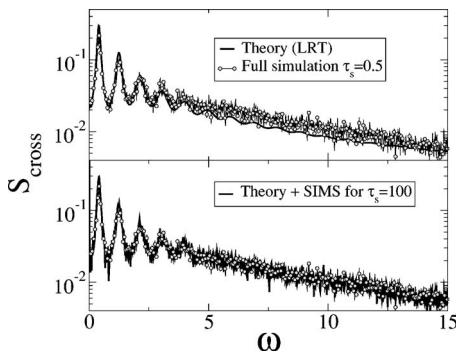


FIG. 5. Improved theory for the cross spectrum for $\mu=0.8$, $D=0.12$, $D_E=0.08$, $G=-1.0$, $\tau_R=0.1$, $\tau_S=0.5$, and $\tau_D=6.324$ (feedback strength and delay have been increased compared to the parameters in Fig. 4). Upper panel: The full simulation result (black) is compared to the purely theoretical result Eq. (34). Lower panel: The same simulation result is compared to Eq. (38) where we have used Eq. (42). The latter cross spectrum was estimated by another network simulation using the parameters above except for the synaptic decay time which we set $\tau_S=10^3$.

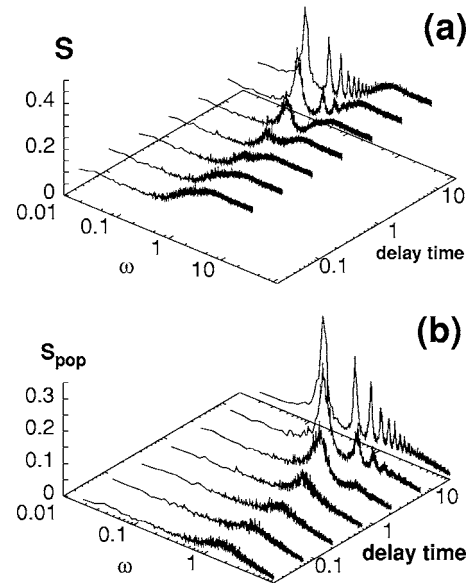


FIG. 6. Spike train power spectrum (a) and spectrum of the network activity (b) for different delay time τ_D and a subthreshold bias current $\mu=0.8$. The data were obtained by numerical simulation of a network with $N=100$. Other parameters: $G=-1.0$, $D=0.12$, $D_E=0.08$, $\tau_R=0.1$, and $\tau_S=0.5$.

Spike train power spectra and spectra of the network activity for different values of the delay time are shown in Figs. 6(a) and 6(b), respectively. For small delay, no network oscillation is present. With increasing delay time ($\tau_D=0.2$), a peak appears both in the power spectrum of the single neuron [Fig. 6(a)] and in the activity spectrum [Fig. 6(b)]. For larger delays ($\tau_D>5$) an increasing number of higher harmonics can be observed. The fundamental frequency decreases with increasing delay time. A similar picture is obtained when the theoretical expressions Eq. (32) and Eq. (35) are plotted against frequency and delay time. A slight quantitative deviation between theory and simulation results is observed at large delay, since the correction of spectra due to the delayed feedback is pretty strong. As typical for a theory with linear corrections, the oscillation is slightly overestimated by the theory. Nevertheless the multi-peaked structure is well reproduced—in Fig. 7 we show the first two peaks of the population spectrum for a delay time of $\tau_D=20$.

The strength of the oscillation can be quantified by the degree of coherence [37,38], i.e., the ratio of peak height and peak-half width, the latter scaled by the peak frequency. Since the spectrum of the population activity shows a much clearer peak than the power spectrum of the spike train (the latter saturates in the high-frequency limit), we consider in the following the degree of coherence of the first (lowest-frequency) peak in the spectrum of the population activity given by

$$\beta = \frac{\omega_{\max} S_{\text{pop}}(\omega_{\max})}{\Delta \omega}, \quad (43)$$

where ω_{\max} and $S_{\text{pop}}(\omega_{\max})$ are the center frequency and height of the first spectral peak, respectively. The difference $\Delta \omega = \omega_R - \omega_L$ is the half-width, i.e., $\omega_{R,L}$ are the closest fre-

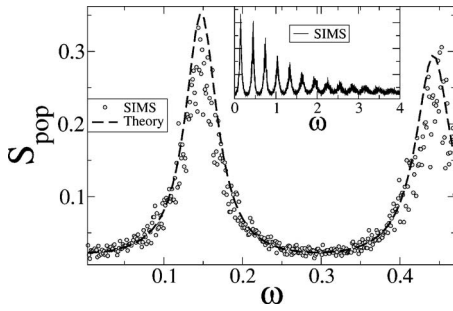


FIG. 7. Power spectrum of the population activity for a large delay time $\tau_D=20$. Symbols are the result of simulations that agree well with theory [solid line, Eq. (35)] except for the peak height which is overestimated by the theory. Other parameters are as in Fig. 6.

quency values to the right and left of ω_{\max} , respectively, for which $S_{pop}(\omega_{R,L})=S_{pop}(\omega_{\max})/2$.

We first consider the oscillation's frequency and the range of frequencies for which the spectrum is above half of the maximum value (of course, the maximum value itself depends on the system's parameters). In Fig. 8(a) we show both the oscillation frequency (solid line) as well as the mentioned frequency range (grey region) as functions of the delay time. The frequency of oscillation [Fig. 8(a)] drops with increasing delay. At small delay, the peak is small and its location is strongly determined by the frequency dependence of the susceptibility and by the synaptic time scale τ_S . For large delay the system oscillates with a period of twice the delay ($\omega_{\max} \rightarrow \pi/\tau_D$)—this asymptotic limit is shown by a dashed line and becomes particularly clear in the log-log plot in the inset of Fig. 8(a). The peak width also decreases with delay time. Together with the increase in height of the spectral peak with growing delay, we thus obtain a monotonically increasing degree of coherence [cf. Fig. 8(b)].

That the oscillation becomes more pronounced with increasing delay time is mainly due to the synaptic filtering included in the feedback. At short delay, no sharp delayed activity is received by the network due to the effect of the α function. The larger the delay is, the more diminished is the effect of the synapse. We also note that, for the small base current μ we have chosen, no pronounced intrinsic frequency is present, so the oscillation peak is mainly determined by the network properties, i.e., delay time τ_D and synaptic time scale τ_S . Remarkably, in the large-delay limit, the ratio of peak width and peak frequency approaches a constant. The same holds true for the height of the first peak. Consequently, according to Eq. (43), the degree of coherence saturates for large τ_D . Although the agreement between the predictions of the theory and the simulation results is generally satisfying, the theory overestimates the degree of coherence at large delay time. Since the peak height is slightly overestimated, the width of the peak will also be underestimated. Therefore, the slight disagreement seen in the theoretical and simulation spectra (cf. Fig. 7) leads to a fairly large error in β .

We now turn to the effect of varying the internal noise intensity D . In Fig. 9 we show how the spectra evolve with the internal noise intensity D instead of the delay time. At low internal noise, a pronounced peak is apparent both in the

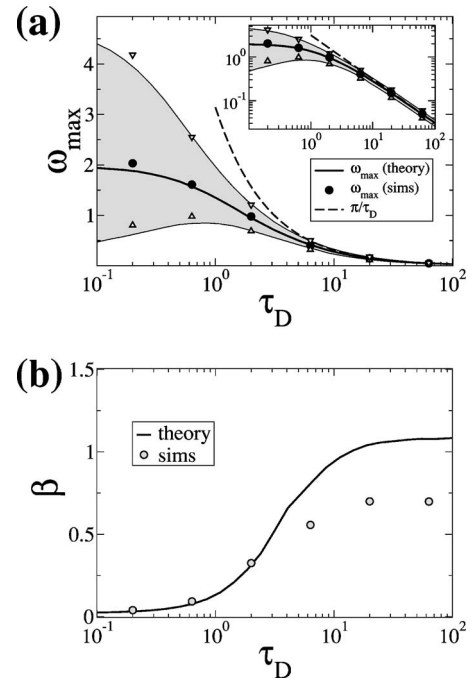


FIG. 8. Oscillation frequency (a) and spectral coherence (b) of the first peak in the power spectrum of the network activity vs delay time τ_D . The width of the first peak in panel (a) is indicated by the grey area and is defined by $S(\omega) > S(\omega_{\max})/2$. Theoretical curves have been obtained by numerical evaluation of the analytical expression Eq. (35). Simulation results were obtained by smoothing the simulation spectra sufficiently by running averages (length of average depends on system's parameters) and estimating the oscillation frequency and peak width by eye. The dashed line shows the angular frequency that corresponds to twice the delay time (π/τ_D)—this frequency is approached by the oscillation frequency at large delay as seen in the log-log plot in the inset. Parameters are $D=0.12$, $G=-1.0$, $\mu=0.8$, $\tau_R=0.1$, $D_E=0.08$, and $\tau_S=0.5$.

power spectrum of the spike train and in the spectrum of the population activity. With increasing internal noise, the spike train spectrum shows an overall increase due to the increase in firing rate. The peak, however, becomes less pronounced and vanishes even in the strong noise limit. In the activity spectrum the peak remains roughly at the same frequency, decreases and becomes broader with growing D . The evolution of the spectra show that internal noise just adds incoherent spiking unrelated to the delayed feedback. The “optimal” internal noise intensity with respect to the oscillation is zero. There is no stochastic-resonance-like effect present in the system—at least not for the parameter sets we have inspected.

It is of course possible to increase the overall spike rate by increasing the internal noise intensity D . The feedback-induced modulation of the spike rate (leading to the peak at finite frequency) is solely due to the common part of the external noise $\eta_c(t)$. Decreasing or increasing the latter will lead to the opposite effect, namely, a decrease and increase of the peak height and coherence, respectively.

The above observations are also quantitatively confirmed when we look at the degree of coherence depicted in Fig. 10. First of all, an increase in internal noise intensity does not

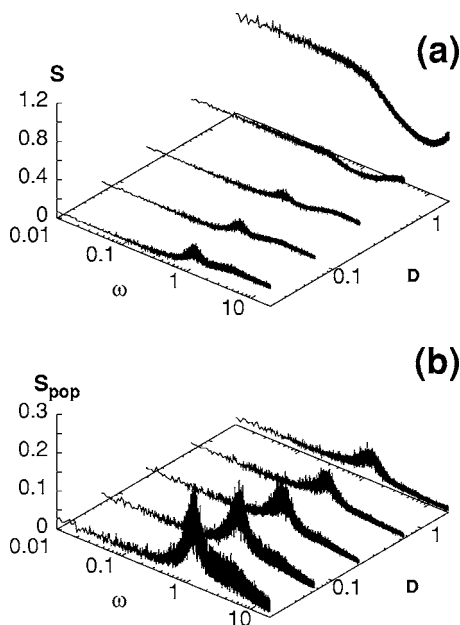


FIG. 9. Spike train power spectrum (a) and spectrum of the network activity (b) for different intensities of the internal noise and subthreshold bias current $\mu=0.8$, obtained by numerical simulation of a network with $N=100$. Other parameters: $D_E=0.08$, $G=-1.0$, $\tau_D=1$, $\tau_R=0.1$, and $\tau_S=0.5$.

change the oscillation frequency drastically; further, the width becomes only marginally wider with increasing D . Both changes are solely due to the dependence of the susceptibility on the internal noise intensity. Second, the degree of coherence [cf. Fig. 10(b)] is maximal in the zero internal noise limit $D=0$. The theory overestimates β , in particular at small internal noise intensity. We note that in this limit the assumptions we have made for deriving our theory are formally violated. A linearization of the single neuron dynamics as assumed in our ansatz Eq. (18) is only given for at least moderate internal noise. However, since we incorporated the external noise in the theory as an internal one, we still obtain a reasonable agreement between theory and simulations.

So far we have considered the subthreshold (“noise-activated”) firing regime of the single LIF neuron, where both the original base current μ as well as the effective base current μ' are so small ($\mu, \mu' < v_T$) that firings are solely due to internal and/or external noise. In this regime, the neuron does not show any pronounced intrinsic eigenfrequency and, consequently, the observed feedback-induced time-scale was merely determined by the network parameters τ_D and τ_S .

Increasing the bias current such that $\mu, \mu' > 1$ and decreasing the total noise strength Q will result in a pronounced eigenfrequency of the neuron. In this case, will there be any interaction between the delayed feedback and the intrinsic time scales? This question is addressed in Fig. 11 where we show power spectra of the spike train and of the network activity for a suprathreshold base current and different values of the delay time. As in the noise-activated firing regime, a small value of the delay time does not lead to a feedback-induced peak. The peak which is present in the power spectrum of the spike train is that due to the spontaneous activity at the eigenfrequency of the LIF neuron. For

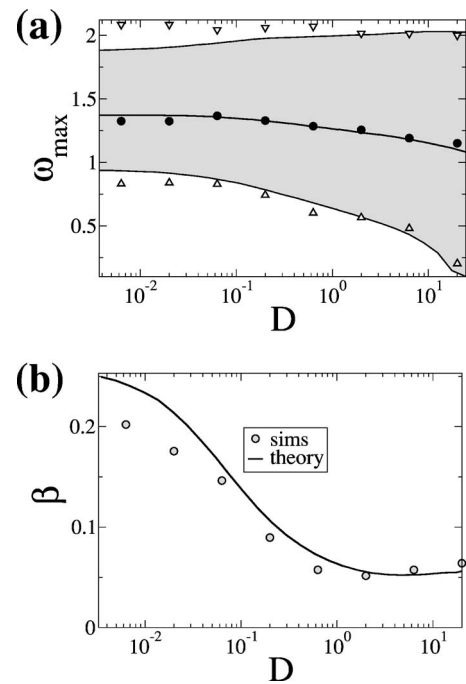


FIG. 10. Oscillation frequency (ω_{max}) and width of the first peak [peak area is grey and is defined by $S(\omega) < S(\omega_{max})/2$] in the spectrum of the population activity as a function of the internal noise intensity. Theoretical curves have been obtained by numerical evaluation of the analytical expression Eq. (35). Simulation results were obtained by smoothing the simulation spectra sufficiently by running averages (length of average depends on system’s parameters) and estimating the oscillation frequency and peak width by eye. Parameters are $D_E=0.08$, $G=-1.0$, $\mu=0.8$, $\tau_R=0.1$, $\tau_D=1$, and $\tau_S=0.5$.

moderate delay time ($\tau_D=0.2$) a peak emerges that grows in height and shifts to lower frequencies as we increase τ_D . At large delay, we observe a qualitative difference in comparison to the subthreshold case: the peak at the basic frequency drops in height, whereas the higher harmonic that is closest to the eigenfrequency of the neuron is stronger than the basic frequency. Note that according to our theory, we can expect such an observation since, for an LIF neuron in the suprathreshold firing regime, the susceptibility is a nonmonotonic function of the frequency with a strong peak at the neuronal eigenfrequency. Indeed, plotting the theoretical expressions yields a very similar picture to that in Fig. 11 (not shown).

It is evident that in the suprathreshold case, quantifying the oscillation only by the basic frequency would yield a nonmonotonic degree of coherence as a function of the delay time. This would not be so, however, if the highest peak in the activity spectrum were considered.

C. Large network: Synchrony in the network

In the case of a correlated input ($c=1$) there are two possible sources of synchronized activity. First, the neuronal firings can be partially synchronized via the common input even in the absence of feedback. This is easily seen in the limit of a vanishing internal noise and vanishing feedback ($D=0, G=0$) where the firing of the neurons becomes en-

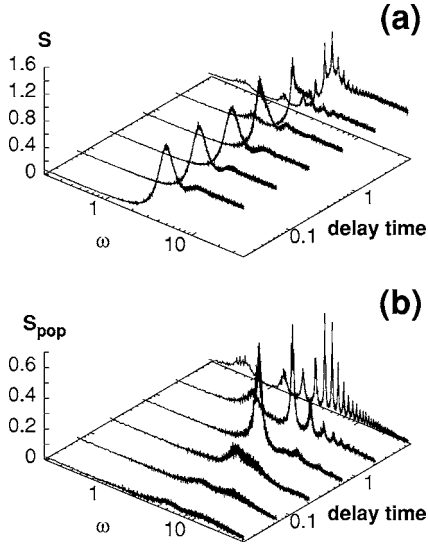


FIG. 11. Spike train power spectrum (a) and spectrum of the network activity (b) for different values of the delay time τ_D and *suprathreshold* bias current $\mu=1.7$, lower noise and smaller synaptic time scale than in the previous figures. Parameters are $D=0.025$, $D_E=0.025$, $G=-0.5$, $\tau_R=0.1$, and $\tau_S=0.05$.

tirely synchronized. Secondly, in case of a feedback-induced oscillation, the spiking of the neurons is also locked in a stochastic manner to this oscillation, and the spikes of two arbitrary neurons will be correlated through this oscillation. Here we consider the second form of synchronization between spike trains by means of the correlation function in the time domain.

For finite τ_S the correlation functions are well described by the theory as shown in Figs. 12(a) and 12(b). Remarkably, at the large delay time we have chosen in this numerical example, the part of the graph corresponding to the correlation- and feedback-induced oscillation is the same for auto and cross correlation functions. This is similar to the cases of excitability- and latency-induced cross correlation in Ref. [39]. We recall that the spike-spike correlation function can be interpreted as the probability with which a spike occurs at time $\tau \neq 0$ given there was a spike at $\tau=0$. For the auto correlation function the reference spike at $\tau=0$ belongs to the same spike train whereas for the cross correlation function it belongs to the spike train of the second neuron. The closeness of both correlation functions to each other at larger τ indicates that the cross- and autocorrelation in this range are solely due to the common correlation of both spike trains to the feedback kernel. This can also be extracted from the theory as follows. Subtracting the cross spectrum between distinct spike trains Eq. (34) from the power spectrum of a single spike train Eq. (32), we obtain

$$S - S_{cross} = S_{0,Q} - 2cD_E|A_Q|^2, \quad (44)$$

an expression that does not involve the feedback kernel $F(\omega)$ anymore. This implies that the difference of auto and cross correlation functions does not contain any dependence on the delay time (this difference equals the Fourier transform of

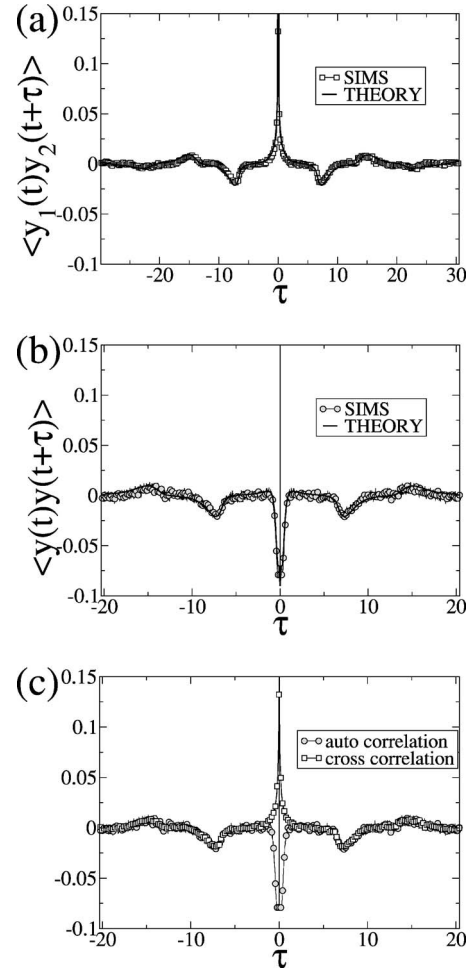


FIG. 12. Auto- and cross-correlation functions of single neuron spike trains for a large network with $N=100$. (a) Cross correlation of two spike trains from distinct neurons. Simulation (grey circles) are compared to theory [solid line, numerically calculated inverse Fourier transform of Eq. (34)]. The cross correlation shows minima and maxima at multiples of the delay time $\tau_D=6.324$. (b) Autocorrelation function. Simulations (grey circles) vs theory [solid line, numerically calculated inverse Fourier transform of Eq. (32)]. Again minima and maxima are observed at multiples of $\tau_D=6.324$. (c) Comparison of the simulation data for cross- (solid line) and autocorrelation functions. Note that both differ only for small τ but agree well at the oscillation-induced peaks at multiples of the delay time $\tau_D=6.324$.

the difference between auto and cross spectra) and, hence, no signature of the network oscillation.

V. SUMMARY

In this paper we have developed a simple theory for spectral measures of spiking stochastic neurons in a network with delayed feedback coupling. We have shown that oscillatory spiking activity in a large network can result from the combination of a shared noisy input (with no specific time scale) and an internal network delayed feedback. We saw that the oscillation for neurons in the subthreshold (noise-activated) firing regime is most pronounced at low internal noise and

long delay. In contrast, in the supra-threshold (intrinsic oscillation) firing regime the optimal delay time (with respect to the network oscillation strength) is—in a certain sense—not at infinity but at a value that corresponds to the inverse intrinsic eigenfrequency of the neuron. At larger delay time, a high anharmonicity of the oscillation occurs—the highest spectral peak is not necessarily at the fundamental frequency of the oscillation but at the higher harmonic which is closest to the eigenfrequency of the neuron.

Finally, we showed that the synchronized activity due to the feedback-induced oscillation correlates spikes within the same spike train and in different spike trains in a similar way. This is comparable to two neurons that are driven by the same external periodic signal, or by two neurons whose excitability levels are covaried in time [39]. At short time scales, auto- and cross-correlations will be different due to the refractory period of the single neuron. At larger time, however, firings of the two neurons and the firings of one and the same neuron will be correlated in exactly the same way, namely, through the phase of the external signal.

To date, many past theoretical treatments of network dynamics properly account for a stochastic forcing where the time-dependent input statistics are synchronously covaried across the population [16–22,22–24]. However, by necessity of the stochastic mean field treatment, all these studies require that the specific membrane fluctuations are uncorrelated between separate neurons in the population. Surprisingly, relatively few studies have considered the impact of shared fluctuations across the population (see the Introduction for references). Our quantitative theory is a perturbative treatment where we have focused on the small shared fluctuation case, even though in practice our predictions hold well with moderately large shared fluctuations (we note that even for $c=1$ the shared fluctuations are still not complete since the intrinsic noise is assumed moderate). The regime of

small (but nonzero) shared fluctuation is perhaps a relevant case for most neural systems. It is well known that synaptic release is unreliable [40], and there is growing evidence that the connectivity within cortical assemblies is sparse [41,42]. However, even small overlapping projections can support nontrivial effects in feed-forward cortical systems [43], and shared fluctuations due to network dynamics have been measured *in vivo* in auditory cortex [9]. These observations suggest that while it is unlikely that two neurons receive completely correlated inputs, interesting and important results may occur when even small shared fluctuations are considered.

We believe that the applicability of our theory is much wider than the framework of the presented material and the reader is encouraged to use some of the techniques revealed here for other neural network phenomena. For instance, the signal transmission of the correlated part of the input noise through the spike train of a single neuron or through the population activity has yet to be addressed. Also, it would be straightforward to extend the analysis to the case of a mixed excitatory and inhibitory feedback. Further, the restriction of a homogeneous network can be relaxed when the spectral equations are averaged with respect to a prescribed distribution of parameter values. The open issues in our analytical results are not so much related to the network problem but to unknown characteristics of the single neuron. It would be, for instance, satisfying to know the cross spectrum of two uncoupled LIF neurons that are driven by independent and correlated noise sources. This elementary problem is, to the authors' knowledge, still unsolved even for the case of simpler neuron models like the perfect integrate-and-fire (or random-walk) model. Likewise, analytical expressions for the cross spectra between the output spike train and the correlated or uncorrelated noise sources could be incorporated into a more exact theory of the network activity.

-
- [1] R. Ritz and T. Sejnowski, *Curr. Opin. Neurobiol.* **7**, 536 (1997).
- [2] G. Buzsáki and A. Draguhn, *Science* **304**, 1926 (2004).
- [3] W. Singer and C. Gray, *Annu. Rev. Neurosci.* **18**, 555 (1995).
- [4] G. Laurent, *Nat. Rev. Neurosci.* **3**, 884 (2002).
- [5] K. Linkenkaer-Hansen, V. Nikulin, S. Palva, R. Ilmoniemi, and J. Palva, *J. Neurosci.* **22**, 3739 (2004).
- [6] P. Fries, J.-H. Schrder, P. R. Roelfsema, W. Singer, and A. K. Engel, *J. Neurosci.* **22**, 3739 (2002).
- [7] J. Huxter, N. Burgess, and J. O'Keefe, *Nature (London)* **425**, 828 (2003).
- [8] E. Salinas and T. J. Sejnowski, *Nat. Rev. Neurosci.* **2**, 539 (2001).
- [9] M. R. Deweese and A. M. Zador, *J. Neurophysiol.* **92**, 1840 (2004).
- [10] B. Doiron, M. J. Chacron, L. Maler, A. Longtin, and J. Bastian, *Nature (London)* **421**, 539 (2003).
- [11] B. Doiron, B. Lindner, A. Longtin, L. Maler, and J. Bastian, *Phys. Rev. Lett.* **93**, 048101 (2004).
- [12] Electroreception and Electrocommunication: Special Issue of the *J. Exp. Biol.* 202, 1167 (1999), edited by R. W. Turner, L. Maler, and M. B.
- [13] L. Glass and M. C. Mackey, *From Clocks to Chaos: The Rhythms of Life* (Princeton University Press, Princeton, NJ, 1988).
- [14] S. Guillouezic, I. L'Heureux, and A. Longtin, *Phys. Rev. E* **59**, 3970 (1999).
- [15] T. D. Frank and P. J. Beek, *Phys. Rev. E* **64**, 021917 (2001).
- [16] L. F. Abbott and C. van Vreeswijk, *Phys. Rev. E* **48**, 1483 (1993).
- [17] W. Gerstner, *Phys. Rev. E* **51**, 738 (1995).
- [18] N. Brunel and V. Hakim, *Neural Comput.* **11**, 1621 (1999).
- [19] D. J. Mar, C. C. Chow, W. Gerstner, R. W. Adams, and J. J. Collins, *Proc. Natl. Acad. Sci. U.S.A.* **96**, 10450 (1999).
- [20] N. Brunel, *J. Comput. Neurosci.* **8**, 183 (2000).
- [21] W. Gerstner, *Neural Comput.* **12**, 43 (2000).
- [22] B. W. Knight, *Neural Comput.* **12**, 473 (2000).
- [23] M. Mattia and P. Del Giudice, *Phys. Rev. E* **66**, 051917 (2002).
- [24] C. Leibold, *Phys. Rev. Lett.* **93**, 208104 (2004).

- [25] C. Zhou, J. Kurths, and B. Hu, Phys. Rev. Lett. **87**, 098101 (2001).
- [26] H. Busch and F. Kaiser, Phys. Rev. E **67**, 041105 (2003).
- [27] S. Wang, F. Liu, W. Wang, and Y. Yu, Phys. Rev. E **69**, 011909 (2004).
- [28] G. Svirskis and J. Hounsgaard, Network Comput. Neural Syst. **14**, 747 (2003).
- [29] H. Sompolinsky, H. Yoon, K. Kang, and M. Shamir, Phys. Rev. E **64**, 051904 (2001).
- [30] B. Lindner, L. Schimansky-Geier, and A. Longtin, Phys. Rev. E **66**, 031916 (2002).
- [31] B. Lindner and L. Schimansky-Geier, Phys. Rev. Lett. **86**, 2934 (2001).
- [32] P. Hänggi and H. Thomas, Phys. Rep. **88**, 207 (1982).
- [33] B. Lindner, M. J. Chacron, and A. Longtin, Phys. Rev. E **72**, 021911 (2005).
- [34] A. V. Holden, *Models of the Stochastic Activity of Neurones* (Springer-Verlag, Berlin, 1976).
- [35] M. Abramowitz and I. A. Stegun, *Handbook of Mathematical Functions* (Dover, New York, 1970).
- [36] H. Risken, *The Fokker-Planck Equation* (Springer, Berlin, 1984).
- [37] Hu Gang, T. Ditzinger, C. Z. Ning, and H. Haken, Phys. Rev. Lett. **71**, 807 (1993).
- [38] A. Longtin, Phys. Rev. E **55**, 868 (1997).
- [39] C. D. Brody, Neural Comput. **11**, 1537 (1999).
- [40] C. Koch, *Biophysics of Computation - Information Processing in Single Neurons* (Oxford University Press, New York, Oxford, 1999).
- [41] A. Thomson, D. C. West, Y. Wang, and A. P. Bannister, Cereb. Cortex **12**, 936 (2002).
- [42] B. Hellwig, Biol. Cybern. **82**, 111 (2000).
- [43] A. Reyes, Nat. Neurosci. **6**, 593 (2003).